

terminal phosphorus environments. Two chemical shifts and observable P-P coupling for each isomer result. In isomer C, $\Delta\delta$ for the inequivalent phosphorus atoms and the average Ag-P coupling constants are both approximately equal to 100 Hz and combine to produce a pair of overlapping doublet of doublets, which appear as a triplet pattern (Figure 5, $J = +9$ or -9 Hz). Isomer D has ^{31}P chemical shifts more disparate in magnitude ($\Delta\delta$ is approximately 180 Hz with Ag-P coupling of 100 Hz), and the expected doublet of doublets of doublets pattern is observed. The 18-Hz phosphorus-phosphorus coupling constant is read directly from the f_1 axis (Figure 5). The less precise P-P coupling constant value is almost identical for isomers C and D and is within experimental error of the 21-Hz value used to simulate both isomers in the one-dimensional spectrum.

The 100-Hz two-bond Ag-P coupling constants are larger than two-bond couplings found in similar compounds.¹⁹ Two-bond couplings between Ag and a phosphine on a heteroatom are generally unresolved, and the average Ag-P couplings are ca. 8-32 Hz. The 21-Hz P-P coupling in the 3:1 and 4:0 isomers is also high for a four-bond coupling.²⁰ The large through-metal Ag-P and P-P coupling constants in $[\text{AgIr}_2(\text{dimen})_4(\text{PPh}_3)_2](\text{PF}_6)_3$ are likely due to the high symmetry of the complex, the coordination number of 2 for Ag^+ , and the collinear nature of the P-Ir-Ag-Ir-P³⁺ bond vectors.

- (19) (a) Carty, A. J.; Graham, N. M.; Taylor, N. J. *J. Am. Chem. Soc.* **1979**, *101*, 3131. (b) Carty, A. J.; Graham, N. M.; Taylor, N. J. *Organometallics* **1983**, *2*, 447. (c) Freeman, M. J.; Green, M.; Orpen, G.; Salter, I. D.; Stone, F. G. A. *J. Chem. Soc., Chem. Commun.* **1983**, 1332. (d) Ladd, J. A.; Hope, H.; Balch, A. L. *Organometallics* **1984**, *3*, 1838. (e) Rhodes, L. F.; Huffman, J. C.; Caulton, K. G. *J. Am. Chem. Soc.* **1984**, *106*, 6874.
- (20) A marginally applicable example is described for an organophosphorus compound: Grim, S. O. In *Phosphorus-31 NMR Spectroscopy in Stereochemical Analysis*; Verkade, J. G., Quin, L. D., Eds. VCR Publishers, Inc.: Deerfield Beach, FL, 1987; p 650. To our knowledge, no four-bond, through-metal P-P coupling constants have been observed.

The chemical shifts of isomer A-D (the 2:2 cis and trans isomers) of -14.77 and -14.45 ppm, respectively, are close to the average of the two phosphorus chemical shifts in the 3:1 (-14.7 ppm) and 4:0 (-14.85 ppm) isomers. It is useful to realize that as the dimen ligands in the 2:2 isomers are reversed one by one to yield first the 3:1 and then the 4:0 isomer, the chemical shifts of the inequivalent phosphorus atoms diverge. One end of the P-Ir-Ag-Ir-P unit progressively becomes more crowded as the bulkier dimethyl-substituted ends of the dimen ligands bind to the same side of the molecule. In the extreme case of the 4:0 isomer, one terminal phosphine ligand is adjacent to four methyl groups while the other terminal phosphine ligand is exposed to eight methyl groups.

The interconversion rate of the four isomers is slow on the ^{31}P NMR time scale. The sharpness of the individual peaks in the complex multiplet at -14.7 ppm indicates that fluxional processes which involve the dissociation of triphenylphosphine from the axial positions are slow. The compound is robust in solution, and no free triphenylphosphine is observed in the ^{31}P NMR spectrum. When 1 additional equiv of triphenylphosphine is added to a solution of the complex, no changes in the relative sizes of peaks in the -14.7 ppm multiplet are observed. We do observe two small, unresolved peaks in the ^{31}P NMR spectrum (P bound to Ir at -40 ppm, broad; P bound to Ag at 11 ppm, broad), which we attribute to a complex that contains a Ag-PPh₃ unit bound outside of the iridium-dimen cage (i.e. a complex with a P-Ir-Ir-Ag-P³⁺ unit). The isolation and characterization of this complex and additional group 1B analogue chemistry will be the subject of a future report.

Acknowledgment. We thank Doyle Britton and Steve Philson for several stimulating discussions and Johnson-Matthey, Inc., for a generous loan of iridium trichloride.

Supplementary Material Available: Tables SI, SII, and SIV, listing crystallographic data, thermal parameters, and intramolecular distances (10 pages); Table SIII, giving observed and calculated structure factors (9 pages). Ordering information is given on any current masthead page.

Contribution from the Department of Chemistry and Biochemistry, University of Notre Dame, Notre Dame, Indiana 46556

Direct Determination of the Self-Exchange Rate of a Nickel(IV/III) Bis(oxime-imine) Complex. Investigation of Orientation Effects in Electron-Transfer Reactions

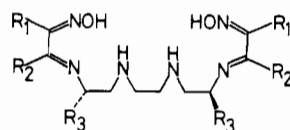
Rosemary A. Marusak, Christopher Sharp, and A. Graham Lappin*

Received February 27, 1990

The electron self-exchange rate for the couple $[\text{Ni}^{\text{IV/III}}\text{Me}_2\text{L}(1)]^{2+/+}$ ($\text{Me}_2\text{L}(1)\text{H}_2 = 3,14$ -dimethyl-4,7,10,13-tetraazahexadeca-3,13-diene-2,15-dione dioxime) has been determined as $2.4 \times 10^4 \text{ M}^{-1} \text{ s}^{-1}$ at 25 °C and 0.10 M ionic strength by ^1H NMR line broadening. Rate constants for cross-reactions calculated with use of this self-exchange rate in the Marcus relationship show good agreement with measured values. The effect of the paramagnetic ions $[\text{Cr}(\text{edta})]^-$, $[\text{Ni}^{\text{III}}\text{Me}_2\text{L}(1)]^+$, and $[\text{Cr}(\text{phen})_3]^{3+}$ on the ^1H NMR relaxation rates of the cobalt(III) complex $[\text{Co}^{\text{III}}\text{Me}_2\text{L}(1)]^+$ has been used to investigate ion-pair structure in solution. These ion pairs serve as models for the electron-transfer precursor assemblies in the self-exchange reaction and two cross-reactions, respectively. Marcus calculations are relatively insensitive to the precursor structures. However, these structures provide a basis for interpretation of stereoselectivity data.

Introduction

The nickel complex $[\text{Ni}^{\text{IV}}\text{Me}_2\text{L}(1)]^{2+}$, where $\text{Me}_2\text{L}(1)\text{H}_2 = 3,14$ -dimethyl-4,7,10,13-tetraazahexadeca-3,13-diene-2,15-dione dioxime (1), has a reduction potential¹ of 0.66 V and is a useful



- I
- $\text{R}_1\text{R}_2\text{L}(1)\text{H}_2$ ($\text{R}_3 = \text{H}$)
 $\text{R}_1\text{R}_2\text{L}(2)\text{H}_2$ ($\text{R}_3 = \text{CH}_3$)
 $\text{R}_1\text{R}_2\text{L}(3)\text{H}_2$ ($\text{R}_3 = \text{CH}_2\text{C}_6\text{H}_5$)

outer-sphere electron-transfer reagent.¹⁻⁵ Application of the Marcus relationship to cross-reactions with a number of reaction partners leads to estimates for the $[\text{Ni}^{\text{IV/III}}\text{Me}_2\text{L}(1)]^{2+/+}$ self-exchange rate from 1×10^4 to $9 \times 10^4 \text{ M}^{-1} \text{ s}^{-1}$.⁴ A pseudo-self-exchange rate has been determined as $6 \times 10^4 \text{ M}^{-1} \text{ s}^{-1}$ from the cross-reaction of $[\text{Ni}^{\text{III}}\text{Me}_2\text{L}(1)]^+$ with $[\text{Ni}^{\text{IV}}\text{Me}_2\text{L}(2)]^{2+}$, a complex with the structurally similar³ chiral ligand. In this paper,

- (1) Lappin, A. G.; Laranjeira, M. C. M. *J. Chem. Soc., Dalton Trans.* **1982**, 1861-1865.
 (2) Macartney, D. H.; McAuley, A. *Inorg. Chem.* **1983**, *22*, 2062-2066.
 (3) Lappin, A. G.; Laranjeira, M. C. M.; Peacock, R. D. *Inorg. Chem.* **1983**, *22*, 786-791.
 (4) Lappin, A. G.; Martone, D. P.; Osvath, P. *Inorg. Chem.* **1985**, *24*, 4187-4191.
 (5) Lappin, A. G.; Martone, D. P.; Osvath, P.; Marusak, R. A. *Inorg. Chem.* **1988**, *27*, 1863-1868.

the self-exchange reaction of $[\text{Ni}^{\text{IV}}\text{Me}_2\text{L}(1)]^{2+}$ is determined by NMR line broadening.

Outer-sphere electron-transfer reactions occur in two distinct steps; a diffusion process in which the reaction partners are assembled in a precursor complex and the rate-limiting electron-transfer process itself. It has been proposed³⁻⁷ that structure in the precursor assembly has an important role in determining chiral induction in electron-transfer reactions of $[\text{Ni}^{\text{IV}}\text{Me}_2\text{L}(2)]^{2+}$ with $[\text{Co}(\text{edta})]^{2-}$ and $[\text{Co}(\text{phen})_3]^{2+}$. Information about steric and electronic constraints on the precursor assembly can be deduced indirectly from examination of discrepancies between experimental and Marcus calculated reaction rates, and this is facilitated by accurate measurements of the $[\text{Ni}^{\text{IV}/\text{III}}\text{Me}_2\text{L}(2)]^{2+/+}$ self-exchange rate. In addition, where the precursor has substantial thermodynamic stability, direct structural information can be obtained from ^1H NMR relaxation studies on model systems. In the presence of a paramagnetic complex, the relaxation rates of ligand ^1H 's in a diamagnetic complex experience a dipolar interaction that is dependent on the distance from the paramagnetic center. This technique for structure elucidation is particularly suited to systems where the symmetry of complexes is low. Because of the limited stability of $[\text{Ni}^{\text{IV}}\text{Me}_2\text{L}(1)]^{2+}$, the complex $[\text{Co}^{\text{III}}\text{Me}_2\text{L}(1)]^+$ is used as a diamagnetic isostructural analogue.⁸ Chromium(III) analogues of $[\text{Co}(\text{edta})]^{2-}$ and $[\text{Co}(\text{phen})_3]^{2+}$ are used as paramagnetic probes in structure elucidation.

Experimental Details

$[\text{Ni}^{\text{IV}}\text{Me}_2\text{L}(1)][\text{ClO}_4]_2$ was prepared by the oxidation of $[\text{Ni}^{\text{II}}\text{Me}_2\text{L}(1)\text{H}_2][\text{ClO}_4]_2$ with cold concentrated HNO_3 .⁹ The nickel(III) form was generated in situ by the addition of the nickel(II) complex at pH ~ 5.5 .⁴ Solutions for NMR self-exchange rate studies were prepared in $\text{D}_2\text{O}/\text{CD}_3\text{COOD}$ (0.02 M) buffer, pH* 5.5, at 0.10 M ionic strength (NaN_3O_3). Fresh nickel(IV) solutions were prepared for each experimental run, and concentrations were determined spectrophotometrically ($\epsilon_{500} = 6300 \text{ M}^{-1} \text{ cm}^{-1}$)⁹ immediately prior to use. The nickel(II) concentration was also determined spectrophotometrically ($\epsilon_{500} = 73 \text{ M}^{-1} \text{ cm}^{-1}$).⁹ Spectra of the nickel(IV) complexes were obtained at 25 °C on a Nicolet NT 300-MHz NMR spectrometer, and transverse relaxation times (T_2) were estimated from peak widths at half-height for the ligand methyl signals. Data acquisition was limited, since significant line broadening due to decomposition of nickel(IV) occurred within 30 min of sample preparation. The data were analyzed on a General Electric 1280 data station equipped with a GEN NMR data processing program.

The cobalt(III) complex $[\text{Co}^{\text{III}}\text{Me}_2\text{L}(1)\text{H}][\text{ClO}_4]_2$ was prepared according to the published procedure.⁸ The absorption spectrum of this complex is independent of pH in the range 2–7 with a shoulder at 302 nm ($\epsilon_{302} = 11\,000 \text{ M}^{-1} \text{ cm}^{-1}$) and a maximum at 257 nm ($\epsilon_{257} = 30\,000 \text{ M}^{-1} \text{ cm}^{-1}$). Below pH 1, the maximum at 257 nm shifts to 264 nm ($\epsilon_{264} = 18\,000 \text{ M}^{-1} \text{ cm}^{-1}$) and is accompanied by slow decomposition. Solutions of the salt are acidic, indicating that the cobalt(III) complex present in neutral solution is $[\text{Co}^{\text{III}}\text{Me}_2\text{L}(1)]^+$, which is protonated with a pK_a around 1. The complex was recrystallized from D_2O several times prior to use in NMR experiments. One- and two-dimensional ^1H NMR spectra for $[\text{Co}^{\text{III}}\text{Me}_2\text{L}(1)]^+$ were run on a Varian VXR 500-MHz spectrometer at 30.0 ± 0.1 °C. Nuclear Overhauser enhancement difference spectra and relaxation experiments were carried out on a General Electric GN or Nicolet NT 300-MHz NMR spectrometer at 25.0 °C.

The symmetry of the $[\text{Ni}^{\text{IV}}\text{Me}_2\text{L}(1)]^{2+}$ complex approximates to C_2 .¹⁰ The ^1H NMR spectrum consists of two well-defined methyl signals (H9, δ 2.05 (s); H8, δ 2.40 (d), $J_{38} = 0.7$ Hz) and six complex methylene multiplets downfield (H7, δ 3.27 (m), $J_{57} = 9.6$ Hz; H6, δ 3.40 (d of d of d), $J_{46} = 13.5$ Hz, $J_{36} = 6.0$ Hz, $J_{26} = 1.5$ Hz; H5, δ 3.54 (m); H4, δ 3.61 (d of d of d), $J_{34} \approx 13$ Hz, $J_{24} = 7.3$ Hz; H3, δ 4.42 (m), $J_{23} = 16.6$ Hz; H2, δ 4.24 (d of d of d)). The amine proton signal (H1) cannot be detected, suggesting rapid exchange with solvent. Peaks were assigned (Figure 1) on the basis of the coupling constants and by comparison with the spectrum of the cobalt(III) analogue (H9, δ 2.24 (s); H8, δ 2.65 (d),

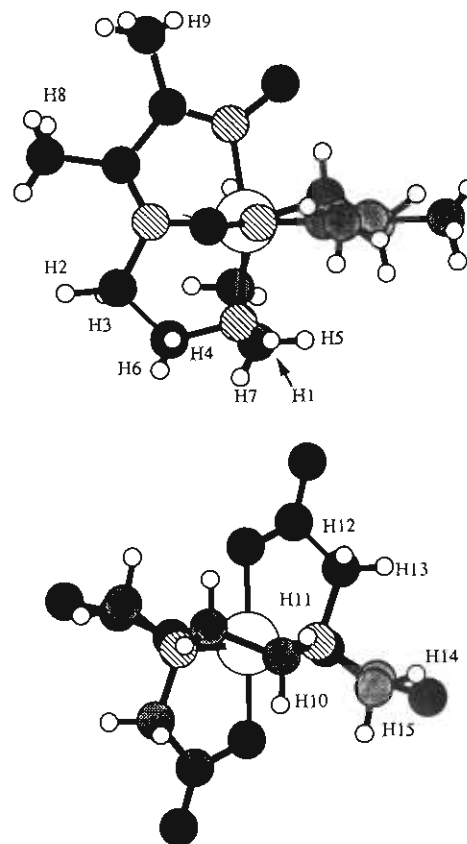


Figure 1. Structure and ^1H assignments for $[\text{Co}^{\text{III}}\text{Me}_2\text{L}(1)]^+$ and $[\text{Co}(\text{edta})]^-$.

$J_{38} \approx 1$ Hz; H7, δ 3.07 (m), $J_{57} = 8.1$ Hz; H6, δ 3.22 (d of d of d), $J_{46} = 13.2$ Hz, $J_{36} = 5.8$ Hz, $J_{26} \approx 2$ Hz; H5, δ 3.33 (m); H4, δ 3.49 (d of d of d), $J_{34} \approx 13$ Hz, $J_{24} = 7.3$ Hz; H3, δ 4.24 (m), $J_{23} = 16.5$ Hz; H2, δ 4.37 (d of d of d); H1, δ 5.90 (s). The longer lifetime of this complex in aqueous solution allows assignment by 2D and nOe experiments. There remains some ambiguity about the assignment of individual proton signals H5 and H7, which show evidence of coupling to the diastereotopic protons as the symmetry is reduced from C_2 .

The complexes $[\text{Cr}(\text{phen})_3]^{3+}$ ($\epsilon_{267} = 65\,700 \text{ M}^{-1} \text{ cm}^{-1}$),¹¹ $\text{Na}[\text{Cr}(\text{edta})]\cdot\text{H}_2\text{O}$ ($\epsilon_{545} = 202 \text{ M}^{-1} \text{ cm}^{-1}$),¹² and $\text{Na}[\text{Co}(\text{edta})]\cdot 4\text{H}_2\text{O}$ ($\epsilon_{535} = 331 \text{ M}^{-1} \text{ cm}^{-1}$)¹³ were prepared according to literature procedures. The complex $[\text{Cr}(\text{edta})]^-$ exists as the hydrated species $[\text{Cr}(\text{edta})(\text{H}_2\text{O})]^-$ below pH 5, but between pH 5 and 9, there is evidence for sixidentate coordination of the ligand with a shift in the visible absorption maximum to 585 nm ($\epsilon_{585} = 200 \text{ M}^{-1} \text{ cm}^{-1}$). ^1H T_1 relaxation experiments were analyzed as described previously.¹⁴ The cobalt(III) concentrations were kept constant at ~ 0.05 M, pH* ≥ 5 , and the paramagnetic complex concentrations ranged $(1.5\text{--}4.0) \times 10^{-4}$ M for $[\text{Cr}(\text{phen})_3]^{3+}$, $(2.0\text{--}16.5) \times 10^{-3}$ M for $[\text{Ni}^{\text{III}}\text{Me}_2\text{L}(1)]^+$, and $(0.4\text{--}2.0) \times 10^{-3}$ M for $[\text{Cr}(\text{edta})]^-$. All solutions were routinely purged with argon to remove any dissolved oxygen, which might affect the observed relaxation rates.

The pH* of the buffer solutions was measured with use of a Beckman Selection 2000 meter equipped with a Corning combination glass electrode with a saturated calomel (NaCl) reference, and the values quoted are uncorrected for isotope effects. Visible spectra were obtained on a Varian DMS 100 spectrophotometer.

Results and Discussion

On addition of $[\text{Ni}^{\text{II}}\text{Me}_2\text{L}(1)]$ to solutions containing an excess of $[\text{Ni}^{\text{IV}}\text{Me}_2\text{L}(1)]^{2+}$, the complex $[\text{Ni}^{\text{III}}\text{Me}_2\text{L}(1)]^+$ is produced rapidly and quantitatively (eq 1).⁴ The methyl signals in the $[\text{Ni}^{\text{IV}}\text{Me}_2\text{L}(1)]^{2+} + [\text{Ni}^{\text{III}}\text{Me}_2\text{L}(1)] \rightarrow 2[\text{Ni}^{\text{III}}\text{Me}_2\text{L}(1)]^+$ (1) nickel(IV) ^1H NMR spectrum provide an excellent monitor for

(6) Martone, D. P.; Osvath, P.; Eigenbrot, C.; Laranjeira, M. C. M.; Peacock, R. D.; Lappin, A. G. *Inorg. Chem.* **1985**, *24*, 4693–4699.

(7) Martone, D. P.; Osvath, P.; Lappin, A. G. *Inorg. Chem.* **1987**, *26*, 3094–3100.

(8) Mohapatra, M.; Chakravorty, V.; Dash, K. C. *Polyhedron* **1989**, *8*, 1509–1515.

(9) Mohanty, J. G.; Singh, R. P.; Chakravorty, A. *Inorg. Chem.* **1975**, *14*, 2178–2183.

(10) Korvenranta, J.; Saarinen, H.; Näsäkkälä, M. *Inorg. Chem.* **1982**, *21*, 4296–4300.

(11) Lappin, A. G.; Segal, M. G.; Weatherburn, D. C.; Sykes, A. G. *J. Am. Chem. Soc.* **1979**, *101*, 2297–2301.

(12) Sawyer, D. T.; McKinnie, J. M. *J. Am. Chem. Soc.* **1960**, *82*, 4191–4196.

(13) Kirschner, S.; Gyarfás, E. C. *Inorg. Synth.* **1957**, *5*, 186–188.

(14) Marusak, R. A.; Lappin, A. G. *J. Phys. Chem.* **1989**, *93*, 6856–6859.

Table I. T_1 Values and Relaxivities for the Interactions of Paramagnetic Complexes with $[\text{CoMe}_2\text{L}(1)]^+$ and $[\text{Co}(\text{edta})]^-$ at 25.0 °C and 0.06 M Ionic Strength

	T_1, s	$R, \text{M}^{-1} \text{s}^{-1}$			$R^{\text{calc}}, \text{M}^{-1} \text{s}^{-1} \text{ }^a$ $[\text{Co}^{\text{III}}\text{Me}_2\text{L}(1)]^+ / [\text{Co}(\text{edta})]^-$
		$[\text{Ni}^{\text{III}}\text{Me}_2\text{L}(1)]^+$	$[\text{Cr}(\text{phen})_3]^{3+}$	$[\text{Cr}(\text{edta})]^-$	
			$[\text{CoMe}_2\text{L}(1)]^+$		
H1	0.473	175 ± 30	280 ± 10	13600 ± 330	13600
H2	0.369	240 ± 10	260 ± 15	8800 ± 310	3700
H3	0.366	180 ± 10	300 ± 11	14000 ± 850	11600
H4	0.358	220 ± 40	270 ± 10	7700 ± 370	2400
H5	0.297	130 ± 20	201 ± 4	15500 ± 630	12000
H6	0.342	180 ± 10	210 ± 15	10600 ± 230	2500
H7	0.378	190 ± 10	210 ± 15	13900 ± 900	12000
H8	0.831	208 ± 10	268 ± 4	5800 ± 200	9500
H9	1.050	280 ± 20	423 ± 4	3000 ± 100	2300
			$[\text{Co}(\text{edta})]^-$		
H10	0.437	408 ± 12			390
H11	0.434	277 ± 10			300
H12	0.509	418 ± 34			410
H13	0.554	698 ± 2			710
H14	0.504	516 ± 9			750
H15	0.513	603 ± 33			600

^aCalculated relaxivities based on the model described in the text. Values were least-squares fit to $\{(1/T_1)_{\text{obsd}} - (1/T_1)_{\text{diam}}\} / [\text{P}] - R_{\text{para}} = \sum A r_{\text{H}(i)}^{-6}$, where A is an empirical constant derived from setting $r_{\text{H1}} = 3.5 \text{ \AA}$. Relaxivities of 900 and $130 \text{ M}^{-1} \text{ s}^{-1}$ were used for R_{para} for $[\text{Cr}(\text{edta})]^-$ and $[\text{Ni}^{\text{III}}\text{Me}_2\text{L}(1)]^+$, respectively. The ionic strength in the $[\text{Co}(\text{edta})]^-$ experiments was 0.25 M.

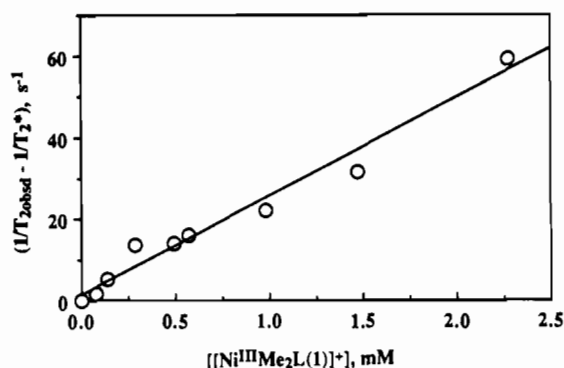


Figure 2. Plot of $((1/T_2)_{\text{obsd}} - 1/T_2^*)$ against $[\text{Ni}^{\text{III}}\text{Me}_2\text{L}(1)]^+$ for line broadening due to electron exchange in the ^1H NMR spectrum of $[\text{Ni}^{\text{IV}}\text{Me}_2\text{L}(1)]^{2+}$ in D_2O , $\text{pH}^* 5.5$ and $25 \text{ }^\circ\text{C}$.

this process, as line broadening occurs in the presence of the paramagnetic ion. The dominant source for this line broadening is the electron-exchange reaction between $[\text{Ni}^{\text{IV}}\text{Me}_2\text{L}(1)]^{2+}$ and $[\text{Ni}^{\text{III}}\text{Me}_2\text{L}(1)]^+$. When no exchange is possible as in the addition of $[\text{Ni}^{\text{III}}\text{Me}_2\text{L}(1)]^+$ to $[\text{Co}^{\text{III}}\text{Me}_2\text{L}(1)]^+$, line broadening by alternative mechanisms is much weaker, about 1% of that due to exchange. The self-exchange rate for $[\text{Ni}^{\text{IV/III}}\text{Me}_2\text{L}(1)]^{2+/+}$, k_{11} , is given¹⁵ by eq 2, where $(1/T_2)_{\text{obsd}}$ and $1/T_2^*$ are the transverse

$$(1/T_2)_{\text{obsd}} = 1/T_2^* + k_{11}[\text{Ni}^{\text{III}}\text{Me}_2\text{L}(1)]^+ \quad (2)$$

relaxation rates, observed and in the absence of the paramagnetic ion, respectively. A plot of $((1/T_2)_{\text{obsd}} - 1/T_2^*)$ against $[\text{Ni}^{\text{III}}\text{Me}_2\text{L}(1)]^+$ is shown in Figure 2, and the self-exchange rate is calculated to be $(2.4 \pm 0.3) \times 10^4 \text{ M}^{-1} \text{ s}^{-1}$ at $25 \text{ }^\circ\text{C}$ and 0.10 M ionic strength. The value, although lower, agrees favorably with the previous estimates of the rate.^{3,4} Comparisons of observed and Marcus calculated rates¹⁶ for the reductions of $[\text{Ni}^{\text{IV}}\text{Me}_2\text{L}(1)]^{2+}$ by $[\text{Co}(\text{edta})]^{2-}$ and $[\text{Co}(\text{phen})_3]^{3+}$, k_{12}^{obsd} (k_{12}^{calcd}), are $36 \text{ M}^{-1} \text{ s}^{-1}$ ($68 \text{ M}^{-1} \text{ s}^{-1}$)^{17,18} and $3.2 \times 10^5 \text{ M}^{-1} \text{ s}^{-1}$ ($1.2 \times 10^5 \text{ M}^{-1} \text{ s}^{-1}$)¹⁹, respectively, both within a factor of 3 and lending credibility to the assignments of outer-sphere mechanisms. Little can be concluded about the requirements for precursor structure from these comparisons. The energetic requirements for electron transfer are substantially greater than those for precursor for-

mation in reactions involving the cobalt(III/II) change.

Although the Marcus calculations are insensitive to variations in precursor structure, ^1H NMR relaxation experiments are capable of providing useful information on structured dipolar interactions between complexes. Where the spectra are complex, it is simpler to investigate the interactions by examining longitudinal relaxation T_1 rather than transverse relaxation T_2 . The dipolar interaction can be expressed as eq 3, where $(1/T_1)_{\text{diam}}$ is

$$(1/T_1)_{\text{obsd}} = M_{\text{diam}}(1/T_1)_{\text{diam}} + M_{\text{para}}(1/T_1)_{\text{para}} + R_{\text{para}}[\text{P}] \quad (3)$$

the relaxation rate in the absence of the paramagnetic ion, P , $(1/T_1)_{\text{para}}$ is the relaxation rate in the isolated, well-structured ion pair, M_{diam} and M_{para} are the mole fractions of the diamagnetic species free and in the ion pair, respectively, and R_{para} is an unstructured outer-sphere paramagnetic relaxivity. When the extent of the ion pairing is small, both paramagnetic terms are linearly dependent on $[\text{P}]$ and are not readily separable. However, for oppositely charged ions, R_{para} is generally small and differences in the relaxivity observed for different ^1H signals can be ascribed to the structured ion-pair term. This structured term can be represented by a simplified Solomon-Bloembergen relationship^{20,21} related as the inverse sixth power to the distance between the nucleus and the paramagnetic center.²²

The ^1H relaxation rates of $[\text{Co}^{\text{III}}\text{Me}_2\text{L}(1)]^+$ as a free ion are presented in Table I. In the presence of the paramagnetic ions $[\text{Ni}^{\text{III}}\text{Me}_2\text{L}(1)]^+$ and $[\text{Cr}(\text{phen})_3]^{3+}$, the rates are increased but effects are relatively small. There is a linear dependence of $1/T_1$ on the concentration of the paramagnetic ion, and the slopes, or relaxivities, indicate that while all the protons on $[\text{Co}^{\text{III}}\text{Me}_2\text{L}(1)]^+$ are not affected to exactly the same extent, the discrimination between the protons is also very small.²³ It is implied that there is little structure in the interactions between the cationic complexes, and hence, the precursor structure imposes no discernible orientational constraints on the subsequent electron transfer. Good agreement with the Marcus theory can be anticipated.

In the presence of $[\text{Cr}(\text{edta})]^-$ the ^1H NMR spectrum of $[\text{Co}^{\text{III}}\text{Me}_2\text{L}(1)]^+$ is affected to a much greater extent than with

(15) Swift, T. J.; Connick, R. E. *J. Chem. Phys.* **1962**, *37*, 307-320.
 (16) Brown, G. M.; Sutin, N. *J. Am. Chem. Soc.* **1979**, *101*, 883-892.
 (17) Ogino, H.; Ogino, K. *Inorg. Chem.* **1983**, *22*, 2208-2211.
 (18) Im, Y. A.; Busch, D. H. *Inorg. Chem.* **1961**, *83*, 3357-3362.
 (19) Warren, R. M. L.; Lappin, A. G.; Mehta, B. D.; Neumann, H. M. *Inorg. Chem.*, in press.

(20) Solomon, I. *Phys. Rev.* **1955**, *99*, 559-565.
 (21) Bloembergen, N. *J. Chem. Phys.* **1957**, *27*, 572-573.
 (22) A complete analysis requires detailed information on the thermodynamics and kinetics of formation of the ion pair and other factors that are not readily obtained.
 (23) The one exception, that H9 is affected greater than the other protons, may be the result of a preferential interaction along the C_2 oxime face of the complex or may be the result of other physical phenomena such as changes in solvation.

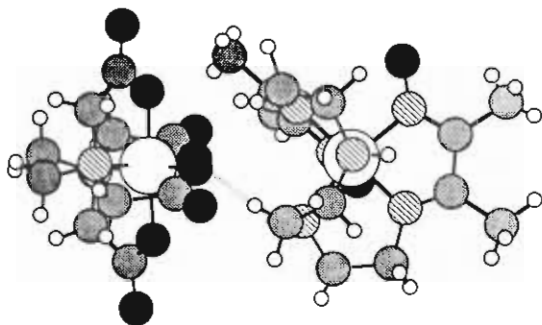


Figure 3. Molecular model representing the structure of the precursor assembly formed between $[\text{Ni}^{\text{IV}}\text{Me}_2\text{L}(1)]^{2+}$ and $[\text{Co}(\text{edta})]^{2-}$. The hydrogen-bonding interaction is shown by the dotted line.

the cationic paramagnetic reagents. The relaxivities show a significant variation depending on the position of the proton on the complex ion. The order of the relaxivities reveals that the protons around the amine proton, H1, are affected to the greatest extent and that the effect diminishes as the distance from this proton increases. Interpretation of these data argues for a hydrogen-bonded interaction through the amine hydrogen atom. In order to elucidate the orientation of the counterion, the effects of the paramagnetic ion $[\text{Ni}^{\text{III}}\text{Me}_2\text{L}(1)]^+$ on protons in $[\text{Co}(\text{edta})]^-$ (Figure 1) were examined. Since $[\text{Ni}^{\text{III}}\text{Me}_2\text{L}(1)]^+$ has a single unpaired electron, relaxivities are smaller than observed in the interaction of $[\text{Cr}(\text{edta})]^-$ with $[\text{Co}^{\text{III}}\text{Me}_2\text{L}(1)]^+$. Relaxivities for carboxylate methylene protons H13, H14, and H15 are enhanced relative to protons H10 and H11 on the ethylenediamine backbone (Table I), suggesting that $[\text{Co}(\text{edta})]^-$ uses a carboxylate face in a hydrogen-bonded interaction with the amine protons of $[\text{Ni}^{\text{III}}\text{Me}_2\text{L}(1)]^+$.

The hydrogen bond between a bound carboxylate oxygen atom on $[\text{Cr}(\text{edta})]^-$ and the amine hydrogen on $[\text{Co}^{\text{III}}\text{Me}_2\text{L}(1)]^+$ establishes a Cr-H(N) distance around 3.5 Å, and hence, the absolute distances of the various protons to the chromium center can be estimated from the relative magnitudes of the relaxivities. Least-squares optimization to the Solomon-Bloembergen equation indicates that the chromium(III) center is located in the plane of one of the oxime-imine chromophores, bisecting the angle between the amine nitrogen and the trans-imine nitrogen, which are also coplanar. The Cr-Co separation is 5.1 Å. There are a number of discrepancies between measured and calculated distances;²⁴ however, the qualitative picture of $[\text{Cr}(\text{edta})]^-$ bound through a hydrogen bond to the amine proton of the ligand is informative. A similar treatment was used in the interaction of $[\text{Ni}^{\text{III}}\text{Me}_2\text{L}(1)]^+$ with $[\text{Co}(\text{edta})]^-$. In this case the paramagnetic

ion is located on the carboxylate face of $[\text{Co}(\text{edta})]^-$ close to the C_2 axis. Consequently, uncertainties are much smaller. A pictorial representation of the model incorporating both complexes is shown in Figure 3.

The precursor ion pair in the reaction of $[\text{Ni}^{\text{IV}}\text{Me}_2\text{L}(1)]^{2+}$ with $[\text{Co}(\text{edta})]^{2-}$ is well defined with evidence for a hydrogen-bonded interaction. It might be expected that the observed rate for the reaction would be greater than that calculated by the Marcus theory, since precursor stability is higher than accounted for in the electrostatic correction.¹⁶ This is not detected, and while it is difficult to attach great significance to this observation, especially since the self-exchange rate for the $[\text{Co}(\text{edta})]^{-/2-}$ system is not well-known,¹⁸ the preferred orientation detected for the ion pair may not be one that is particularly favorable for electron transfer. The observation does indicate relative insensitivity of the Marcus calculations to orientation effects.

The other manifestation of orientation effects in electron-transfer reactions is stereoselectivity. Reduction of $[\Lambda\text{-Ni}^{\text{IV}}\text{Me}_2\text{L}(2)]^{2+}$ by $[\text{Co}(\text{edta})]^{2-}$ produces an enantiomeric excess of 11% $[\Delta\text{-Co}(\text{edta})]^-$, an 11% $\Delta\Lambda$ process,³ and the preferred interaction in models for the precursor ion pair is also $\Delta\Lambda$.⁶ Modification of the ethylenediamine backbone⁶ of the ligand in $[\text{Co}(\text{edta})]^{2-}$ results in stereoselectivities of 11% for $[\text{Co}(\text{pdta})]^-$ ($\text{pdta}^{4-} = 1,2\text{-diaminopropane-}N,N,N',N'\text{-tetraacetate}(4-)$) and 12% for $[\text{Co}(\text{cdta})]^-$ ($\text{cdta}^{4-} = 1,2\text{-diaminocyclohexane-}N,N,N',N'\text{-tetraacetate}(4-)$). The absence of any significant effect on the chiral induction is consistent with the ion-pair structure deduced from NMR studies. Stereoselectivities⁷ for the oxidation of $[\text{Co}(\text{edta})]^{2-}$ by $[\Lambda\text{-Ni}^{\text{IV}}\text{Me}_2\text{L}(2)]^{2+}$ (11% $\Delta\Lambda$), $[\Lambda\text{-Ni}^{\text{IV}}\text{PhMeL}(2)]^{2+}$ (7% $\Delta\Lambda$), and $[\Lambda\text{-Ni}^{\text{IV}}\text{MePhL}(2)]^{2+}$ (21% $\Delta\Lambda$) reveal that replacement of the imine methyl group by a phenyl ring has a much greater influence on the chiral discrimination than replacement of the oxime methyl group, and it is noteworthy that the former group is closer to the seat of interaction for $[\text{Co}(\text{edta})]^{2-}$ on the nickel complex. Similarly, for $[\Lambda\text{-Ni}^{\text{IV}}\text{Me}_2\text{L}(3)]^{2+}$ (22% $\Delta\Lambda$), the substitution of a benzyl for a methyl group at the H3 positions on the methylene backbone substantially affects the site of association.

This model for the precursor complex provides an important structural basis for interpretation of stereoselectivity data. In the reduction of the nickel(IV) complexes by $[\text{Co}(\text{edta})]^{2-}$, it may be concluded that differences in stereoselectivity are the result of differences in chirality at the site of interaction for the reductant, rather than a balance of contributions from pathways of differing chirality as suggested previously.⁷ In the corresponding reductions by $[\text{Co}(\text{phen})_3]^{2+}$, where there is also a strong dependence of stereoselectivity on oxidant structure,⁵ interactions between the complexes are more poorly defined and the stereoselectivity may reflect the requirements of the electron-transfer step²⁵ rather than the precursor complex.

Acknowledgment. We wish to acknowledge the generous financial support of the National Science Foundation (Grant No. CHE 87-02012).

(24) Potential problems include the lability of the ion pair and the fact that observations were made with racemic solutions so that a better model might be expected by considering more than one site for the paramagnetic ion. A further serious complication is the C_2 symmetry of the complex. Since the resulting position of the paramagnetic center lies far from the C_2 axis, each proton signal experiences a proximal and distal interaction that accounts for some of the uncertainty in the computed distances.

(25) Marusak, R. A.; Sharp, C.; Lappin, A. G. *Inorg. Chem.* **1990**, *29*, 2298-2302.